

# Hofstadter butterfly in transition metal dichalcogenide monolayers

*Presenter*

Tran Khoi Nguyen <sup>1</sup>

*Supervisor*

Dr. Huynh Thanh Duc <sup>2</sup>

<sup>1</sup>University of Science, Ho Chi Minh city

<sup>2</sup>Institute of Applied Mechanics and Informatics

Jul, 2025



# Table of Contents

## 1 Overview

## 2 Method

- Three-band tight-binding model without magnetic field
- Three-band tight-binding model under a magnetic field
- Landau levels
- Hall effect

## 3 Summary and Outlook

# Overview

Group VI-B Transition Metal Dichalcogenides (TMD) are compound semiconductors of the type  $\text{MX}_2$

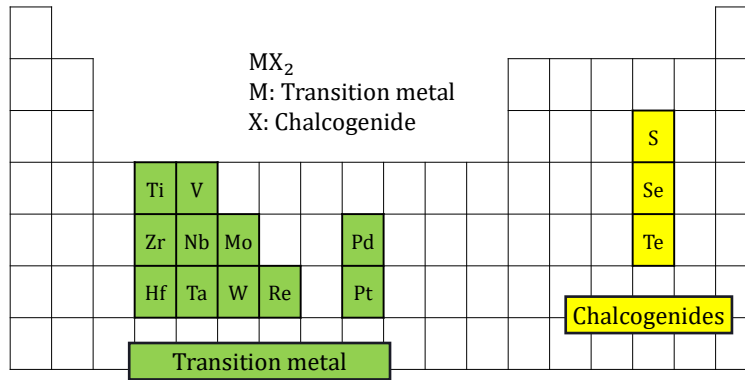
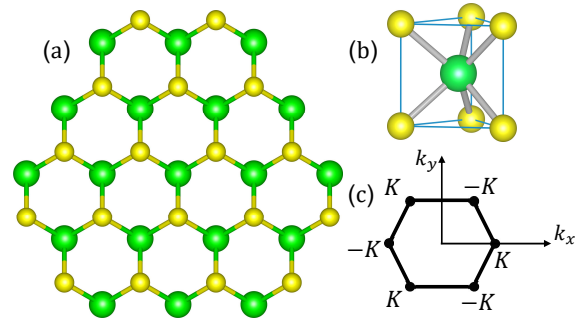


Figure: Transition metal dichalcogenides compound.

# Transition Metal Dichalcogenides Monolayers

- One  $M$  layer sandwiched by two  $X$  layers as shown in top view (a) and side view (b).
- Crystal structure has no central inversion symmetry.
- The symmetry of the lattice results in the hexagon Brillouin Zone (BZ).



**Figure:** Structure and Brillouin Zone of Monolayer TMD<sup>[1]</sup>.

[1] Liu et al., "Three-band tight-binding model for monolayers of group-VIB transition metal dichalcogenides".

# Transition Metal Dichalcogenides Monolayers

## Properties

- Both mono-layer and few-layers remain stable at room temperature.
- TMD monolayer has the visible band gap in the band structure, which can be used in creating the transistor devices<sup>[2]</sup>.
- Strong spin-orbit coupling (SOC) in TMD monolayers lead to spin splitting of hundreds meV.

⇒ Promising material in electronic and optoelectronic applications.

[2] Radisavljevic et al., "Single-layer MoS<sub>2</sub> transistors"

# Three-band tight-binding model without magnetic field

Time-independent Schrödinger equation for an electron in the crystal

$$\left[ -\frac{\hbar^2 \nabla^2}{2m} + U_0(\mathbf{r}) \right] |\psi_{\lambda, \mathbf{k}}(\mathbf{r})\rangle = \epsilon_{\lambda, \mathbf{k}} |\psi_{\lambda, \mathbf{k}}(\mathbf{r})\rangle. \quad (1)$$

Tight-binding (TB) wave function

$$|\psi_{\lambda, \mathbf{k}}(\mathbf{r})\rangle = \sum_j C_j^\lambda(\mathbf{k}) \sum_{\mathbf{R}} e^{i\mathbf{k}\cdot\mathbf{R}} |\phi_j(\mathbf{r} - \mathbf{R})\rangle. \quad (2)$$

The basis consists of three  $d$ -orbitals of the  $M$  atom:

$$|\phi_1\rangle = |d_{z^2}\rangle, |\phi_2\rangle = |d_{xy}\rangle, |\phi_3\rangle = |d_{x^2-y^2}\rangle. \quad (3)$$

The coefficients  $C_j^\lambda(\mathbf{k})$  are the solutions of the eigenvalue equation

$$\sum_{jj'}^3 \left[ H_{jj'}^{\text{TB}}(\mathbf{k}) - \varepsilon_\lambda(\mathbf{k}) S_{jj'}(\mathbf{k}) \right] C_j^\lambda(\mathbf{k}) = 0. \quad (4)$$

# Three-band tight-binding model without magnetic field

Overlap matrix elements

$$S_{jj'}(\mathbf{k}) = \sum_{\mathbf{R}} \langle \phi_j(\mathbf{r}) | \phi_{j'}(\mathbf{r} - \mathbf{R}) \rangle \approx \delta_{jj'}. \quad (5)$$

TB Hamiltonian matrix elements

$$H_{jj'}^{\text{TB}}(\mathbf{k}) = \sum_{\mathbf{R}} e^{i\mathbf{k}\cdot\mathbf{R}} \langle \phi_j(\mathbf{r}) | \left[ -\frac{\hbar^2 \nabla^2}{2m} + U_0(\mathbf{r}) \right] | \phi_{j'}(\mathbf{r} - \mathbf{R}) \rangle. \quad (6)$$

# Three-band tight-binding model without magnetic field

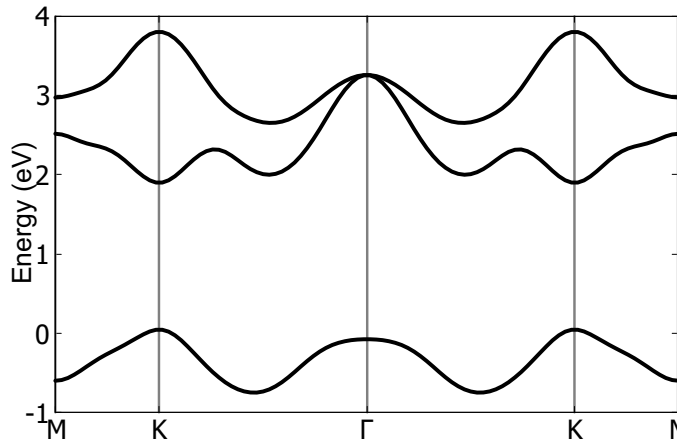


Figure: Band structure of  $\text{MoS}_2$  monolayer<sup>[3]</sup>.

[3] Liu et al., "Three-band tight-binding model for monolayers of group-VIB transition metal dichalcogenides".

# Three-band tight-binding model under a magnetic field

TB Hamiltonian matrix elements change to

$$H = \frac{(-i\hbar\nabla + e\mathbf{A}(\mathbf{r}))^2}{2m} + U_0(\mathbf{r}) + g^*\mu_B\mathbf{B}\cdot\mathbf{L}, \quad (7)$$

It is possible to add a phase factor to the basis functions

$$\psi_{\lambda,\mathbf{k}}(\mathbf{r}) = \sum_{j=1}^3 C_j^\lambda(\mathbf{k}) \sum_{\mathbf{R}} e^{i\mathbf{k}\cdot\mathbf{R}} e^{i\theta_{\mathbf{R}}(\mathbf{r})} \phi_j(\mathbf{r} - \mathbf{R}). \quad (8)$$

By choosing  $\theta_{\mathbf{R}} = -\frac{e}{\hbar} \int_{\mathbf{R}}^{\mathbf{r}} \mathbf{A}(\mathbf{r}') \cdot d\mathbf{r}'$  as Peierls substitution, the Hamiltonian matrix elements as the form

$$\begin{aligned} H_{jj'}^{\text{TB}}(\mathbf{k}) &= \sum_{\mathbf{R}} e^{i\mathbf{k}\cdot\mathbf{R}} e^{\frac{ie}{\hbar} \int_{\mathbf{0}}^{\mathbf{R}} \mathbf{A}(\mathbf{r}') \cdot d\mathbf{r}'} \langle \phi_j(\mathbf{r}) | \left[ -\frac{\hbar^2 \nabla^2}{2m} + U_0(\mathbf{r}) \right] | \phi_{j'}(\mathbf{r} - \mathbf{R}) \rangle \\ &\quad + g^* \mu_B \mathbf{B} \cdot \sum_{\mathbf{R}} e^{i\mathbf{k}\cdot\mathbf{R} + \frac{ie}{\hbar} \int_{\mathbf{0}}^{\mathbf{R}} \mathbf{A}(\mathbf{r}') \cdot d\mathbf{r}'} \langle \phi_j(\mathbf{r}) | \mathbf{L} | \phi_{j'}(\mathbf{r} - \mathbf{R}) \rangle. \end{aligned} \quad (9)$$

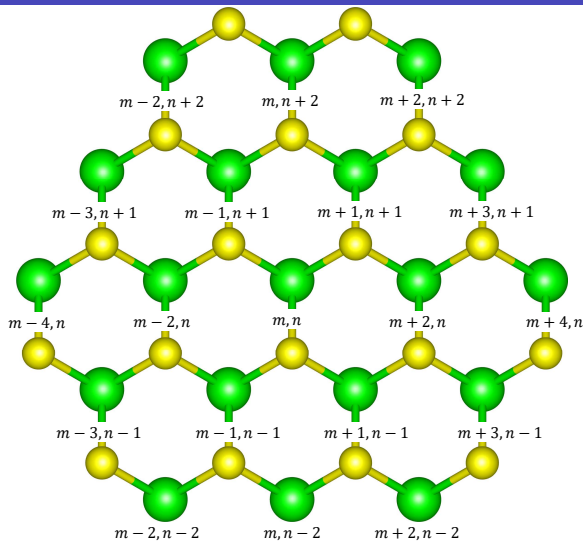


Figure: The TB model of TMDC with six neighbors atom  $M$ .

# Three-band tight-binding model under a magnetic field

The Eq (9) is consist only 1-atom  $M$  in the unit cell, and the Hamiltonian does not invariant under the expansion of lattice vector along the  $x$  axis. In order to restore this invariance, we expanded the origin unit cell into a magnetic unit cell, which now contains 2-atoms  $M$ .

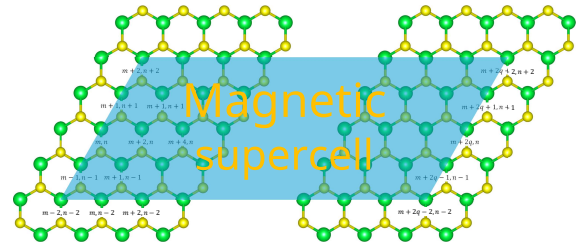


Figure: Magnetic unit cell for TMD monolayers.

# Hamiltonian of magnetic unit cell

The new basis set of  $6q$  atomic orbitals is defined as

$$\psi_{\lambda, \mathbf{k}}(\mathbf{r}) = \sum_{j,i} C_{ji}^{\lambda}(\mathbf{k}) \sum_{\mathbf{R}_{\alpha}}^{N_{UC}} e^{i\mathbf{k}\cdot(\mathbf{R}_{\alpha}+\mathbf{r}_i)} \phi_j(\mathbf{r} - \mathbf{R}_{\alpha} - \mathbf{r}_i), \quad (10)$$

in which  $\mathbf{r}_i$  is the position of an atom in a unit cell, while  $\mathbf{R}_{\alpha}$  is the position of different unit cells. The Hamiltonian matrix elements in the new basis is written as

$$H_{ii'}^{jj'}(\mathbf{k}) = \sum_{\mathbf{R}_{\alpha}}^{N_{UC}} \sum_{\mathbf{R}_{\beta}}^{N_{UC}} e^{i\mathbf{k}\cdot(\mathbf{R}_{\beta}-\mathbf{R}_{\alpha}+\mathbf{r}_{i'}-\mathbf{r}_i)} \langle \phi_j(\mathbf{r} - \mathbf{R}_{\alpha} - \mathbf{r}_i) | \left[ -\frac{\hbar^2 \nabla^2}{2m} + U_0 \right] | \phi_j(\mathbf{r} - \mathbf{R}_{\beta} - \mathbf{r}_{i'}) \rangle. \quad (11)$$

Now we center our system at  $\mathbf{r}' = \mathbf{r} - \mathbf{R}_{\alpha} - \mathbf{r}_i$  and define  $\mathbf{R}_{\gamma} = \mathbf{R}_{\alpha} - \mathbf{R}_{\beta}$ . This lead us to

$$H_{ii'}^{jj'}(\mathbf{k}) = \sum_{\alpha}^{N_{UC}} \sum_{\gamma}^{N_{UC}} e^{-i\mathbf{k}\cdot(\mathbf{R}_{\gamma}+\mathbf{r}_i-\mathbf{r}_{i'})} \langle \phi_j(\mathbf{r}) | \left[ -\frac{\hbar^2 \nabla^2}{2m} + U_0 \right] | \phi_j(\mathbf{r} + \mathbf{R}_{\gamma} + \mathbf{r}_i - \mathbf{r}_{i'}) \rangle. \quad (12)$$

# Hamiltonian of magnetic unit cell

Only considering the nearest-neighbors, we define our hopping terms in the new basis

$$H_{jj'}^{ii'}(\mathbf{k}) = \sum_{\alpha}^{\text{N}_{\text{UC}}} \sum_{\gamma}^{\text{N}_{\text{UC}}} e^{-i\mathbf{k}\cdot\mathbf{R}_{\gamma}} \langle \phi_j(\mathbf{r}) | \left[ -\frac{\hbar^2 \nabla^2}{2m} + U_0(\mathbf{r}) \right] |\phi_{j'}(\mathbf{r} + \mathbf{R}_{\gamma}) \rangle \delta_{i,i'}. \quad (13)$$

Note that  $i = (m, n)$ , taking the sum over  $\mathbf{R}$  and plugging the Peierls phase into Eq. (13), we get the Hamiltonian under a magnetic field

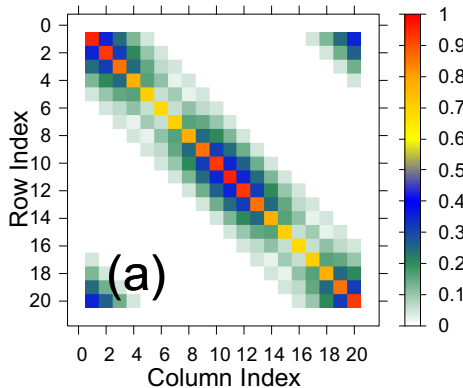
$$H_{jj'}^{ii'}(\mathbf{k}) = e^{\frac{ie}{\hbar} \int_{\mathbf{0}}^{\mathbf{R}} \mathbf{A}(\mathbf{r}') \cdot d\mathbf{r}'} e^{i\mathbf{k}\cdot(\mathbf{0}-\mathbf{R})} \langle \phi_j(\mathbf{r}) | \left[ -\frac{\hbar^2 \nabla^2}{2m} + U_0(\mathbf{r}) \right] |\phi_{j'}(\mathbf{r} - \mathbf{R}) \rangle \delta_{i,i'}. \quad (14)$$

# Hamiltonian of magnetic unit cell

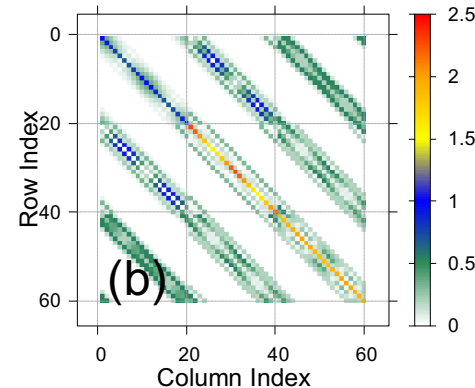
Given the TNN coordinates, the Hamiltonian now invariant and depend on site index  $m, n$ .

$$\begin{aligned}
 H_{jmnj'm'n'}(\mathbf{k}) = & \mathcal{E}_{jj'}(\mathbf{0})\delta_{m,m'}^{n,n'} + e^{i\mathbf{k}\cdot\mathbf{R}_1}\mathcal{E}_{jj'}(\mathbf{R}_1)\delta_{m+2,m'}^{n,n'} + e^{i\mathbf{k}\cdot\mathbf{R}_4}\mathcal{E}_{jj'}(\mathbf{R}_4)\delta_{m-2,m'}^{n,n'} \\
 & + e^{-i\pi(m+1/2)p/q}e^{i\mathbf{k}\cdot\mathbf{R}_2}\mathcal{E}_{jj'}(\mathbf{R}_2)\delta_{m+1,m'}^{n-1,n'} + e^{-i\pi(m-1/2)p/q}e^{i\mathbf{k}\cdot\mathbf{R}_3}\mathcal{E}_{jj'}(\mathbf{R}_3)\delta_{m-1,m'}^{n-1,n'} \\
 & + e^{i\pi(m-1/2)p/q}e^{i\mathbf{k}\cdot\mathbf{R}_5}\mathcal{E}_{jj'}(\mathbf{R}_5)\delta_{m-1,m'}^{n+1,n'} + e^{i\pi(m+1/2)p/q}e^{i\mathbf{k}\cdot\mathbf{R}_6}\mathcal{E}_{jj'}(\mathbf{R}_6)\delta_{m+1,m'}^{n+1,n'} \\
 & + e^{-i\pi(m+3/2)\Phi/\Phi_0}e^{i\mathbf{k}\cdot\tilde{\mathbf{R}}_1}\mathcal{E}_{jj'}(\tilde{\mathbf{R}}_1)\delta_{m+3,m'}^{n-1,n'} + e^{-2i\pi m\Phi/\Phi_0}e^{i\mathbf{k}\cdot\tilde{\mathbf{R}}_2}\mathcal{E}_{jj'}(\tilde{\mathbf{R}}_2)\delta_{m,m'}^{n-2,n'} \quad (15) \\
 & + e^{-i\pi(m-3/2)\Phi/\Phi_0}e^{i\mathbf{k}\cdot\tilde{\mathbf{R}}_3}\mathcal{E}_{jj'}(\tilde{\mathbf{R}}_3)\delta_{m-3,m'}^{n-1,n'} + e^{i\pi(m-3/2)\Phi/\Phi_0}e^{i\mathbf{k}\cdot\tilde{\mathbf{R}}_4}\mathcal{E}_{jj'}(\tilde{\mathbf{R}}_4)\delta_{m-3,m'}^{n+1,n'} \\
 & + e^{2i\pi m\Phi/\Phi_0}e^{i\mathbf{k}\cdot\tilde{\mathbf{R}}_5}\mathcal{E}_{jj'}(\tilde{\mathbf{R}}_5)\delta_{m,m'}^{n+2,n'} + e^{i\pi(m+3/2)\Phi/\Phi_0}e^{i\mathbf{k}\cdot\tilde{\mathbf{R}}_6}\mathcal{E}_{jj'}(\tilde{\mathbf{R}}_6)\delta_{m+3,m'}^{n+1,n'} \\
 & + e^{i\mathbf{k}\cdot\mathbf{R}'_1}\mathcal{E}_{jj'}(\mathbf{R}'_1)\delta_{m+4,m'}^{n,n'} + e^{-2i\pi(m+1)\Phi/\Phi_0}e^{i\mathbf{k}\cdot\mathbf{R}'_2}\mathcal{E}_{jj'}(\mathbf{R}'_2)\delta_{m+2,m'}^{n-2,n'} \\
 & + e^{-2i\pi(m-1)\Phi/\Phi_0}e^{i\mathbf{k}\cdot\mathbf{R}'_3}\mathcal{E}_{jj'}(\mathbf{R}'_3)\delta_{m-2,m'}^{n-2,n'} + e^{i\mathbf{k}\cdot\mathbf{R}'_4}\mathcal{E}_{jj'}(\mathbf{R}'_4)\delta_{m-4,m'}^{n,n'} \\
 & + e^{2i\pi(m-1)\Phi/\Phi_0}e^{i\mathbf{k}\cdot\mathbf{R}'_5}\mathcal{E}_{jj'}(\mathbf{R}'_5)\delta_{m-2,m'}^{n+2,n'} + e^{2i\pi(m+1)\Phi/\Phi_0}e^{i\mathbf{k}\cdot\mathbf{R}'_6}\mathcal{E}_{jj'}(\mathbf{R}'_6)\delta_{m+2,m'}^{n+2,n'}.
 \end{aligned}$$

# Hamiltonian of magnetic unit cell



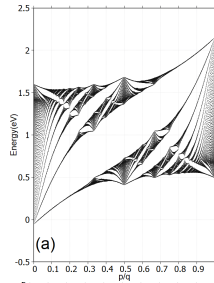
(a)



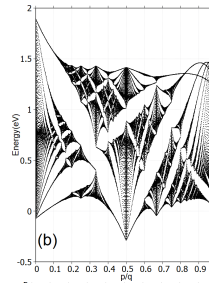
(b)

Figure: An visualization of sub-matrix  $h_0$  for single-band(a) and matrix  $H$  for three band(b) using standard plotter with  $q = 10$ .

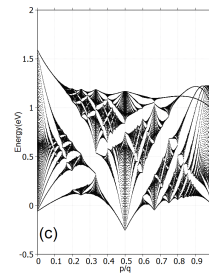
# Hofstadter butterfly<sup>[4]</sup> - Energy band structure



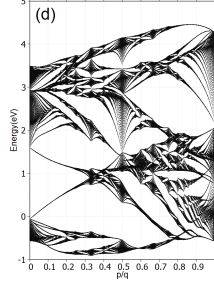
(a)



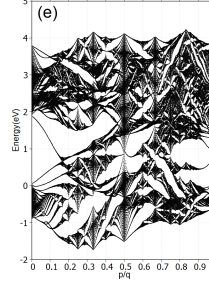
(b)



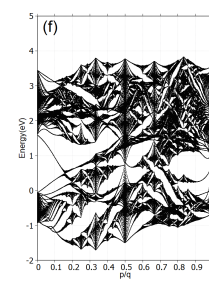
(c)



(d)



(e)

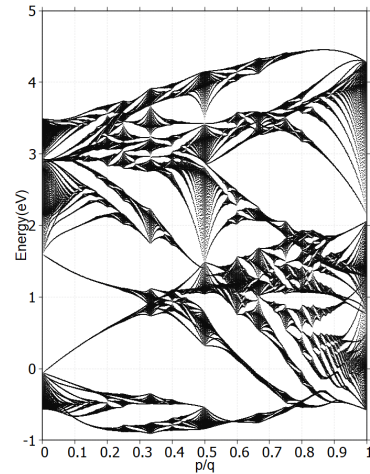


(f)

# Hofstadter butterfly

## Properties

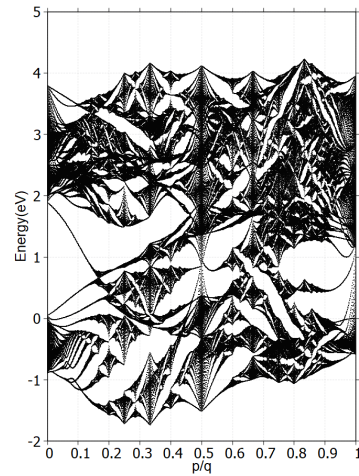
- The spectrum depends only on the flux ratio  $p/q$ .
- The spectrum also invariant under reversal of the magnetic field  $\frac{p}{q} \rightarrow -\frac{p}{q}$ .
- The main energy bands are basically Landau levels
- At weak magnetic field, Landau levels can clearly seen from the Hofstadter spectrum.



# Hofstadter butterfly

## Properties

- The spectrum depends only on the flux ratio  $p/q$ .
- The spectrum also invariant under reversal of the magnetic field  $\frac{p}{q} \rightarrow -\frac{p}{q}$ .
- The main energy bands are basically Landau levels
- At weak magnetic field, Landau levels can clearly seen from the Hofstadter spectrum.



# Hofstadter butterfly with SOC

Three-band TB Hamiltonian under magnetic field with SOC has the form

$$H_{\text{SOC}}(\mathbf{k}) = \begin{pmatrix} H_{3q \times 3q}(\mathbf{k}) + \frac{\lambda}{2} \mathbf{I}_q \otimes L_z & 0 \\ 0 & H_{3q \times 3q}(\mathbf{k}) - \frac{\lambda}{2} \mathbf{I}_q \otimes L_z \end{pmatrix}, \quad L_z = \begin{pmatrix} 0 & 0 & 0 \\ 0 & 0 & 2i \\ 0 & -2i & 0 \end{pmatrix} \quad (16)$$

# Bandstructure of TMD with SOC

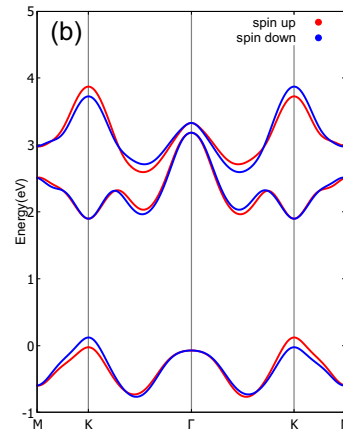
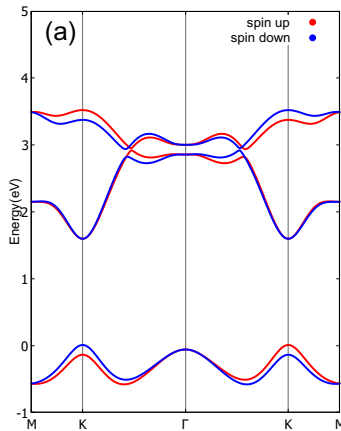


Figure: Band structure of monolayer MoS<sub>2</sub> along  $\Gamma$ -K direction with SOC.

# Hofstadter butterfly with SOC

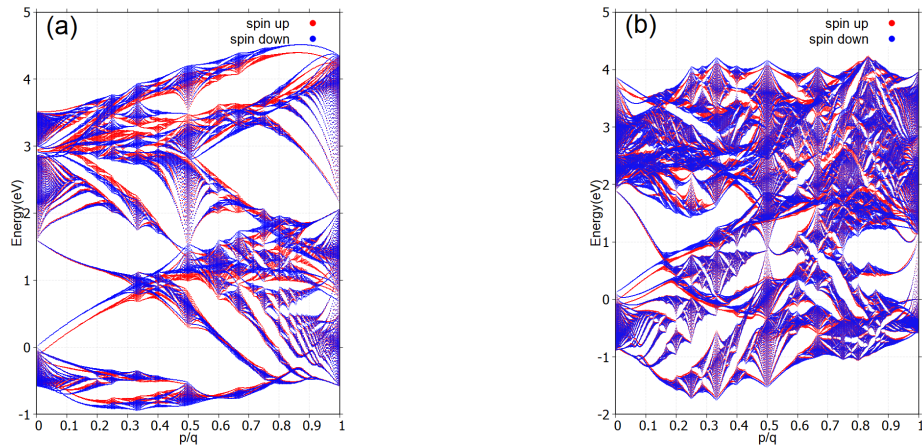


Figure: Hofstadter butterfly with SOC.

# Landau levels

The Hamiltonian for free-electron

$$H = \frac{\mathbf{p} + e\mathbf{A}(\mathbf{r})^2}{2m}, \quad (17)$$

and the energy eigenfunctions are known as Landau levels

$$E_n = (n + 1/2) \hbar \omega_c, \quad (18)$$

where  $\omega_c$  is cyclotron frequency and  $n$  is Landau level index.

# Envelope Function Approximation

The dispersion relation of an electron within TBM

$$H_{11} \approx 6t_0 - \frac{3}{2}t_0 a^2(k_x^2 + k_y^2) + \epsilon_1. \quad (19)$$

Using Envelop Function Approximation (EFA) substitution  $\hbar\mathbf{k} \rightarrow \boldsymbol{\Pi} + e\mathbf{A}$  with Landau gauge  $\mathbf{A} = (0, Bx, 0)$

$$H_{11}(\boldsymbol{\Pi}) \approx 6t_0 - \frac{3}{2}t_0 \frac{a^2}{\hbar^2} \left[ \Pi_x^2 + (\Pi_y + eBx)^2 \right] + \epsilon_1. \quad (20)$$

Eq. (21) can be rewrite in the form as

$$E(\boldsymbol{\Pi}) = 6t_0 - \left[ \frac{1}{2m^*} \Pi_x^2 + \frac{1}{2} m^* \omega_c^2 (x - x_0)^2 \right] + \epsilon_1, \quad (21)$$

where  $m^* = \frac{\hbar^2}{3t_0 a^2}$  is the effective mass and  $x_0 = \frac{\hbar k_y}{eB}$ . Subsequently, the cyclotron frequency is

$$\omega_c = \frac{eB}{m^*} = \frac{8\pi\sqrt{3}t_0}{\hbar} \frac{p}{q}, \quad (22)$$

# Landau Level

and therefore the Landau levels near the bottom of the band structure can be written as

$$\begin{aligned} E_n &= 6t_0 - \hbar\omega_c(n + 1/2) + \epsilon_1 \\ &= t_0 \left( 6 - 8\pi\sqrt{3}\frac{p}{q}(n + 1/2) \right) + \epsilon_1. \end{aligned} \tag{23}$$

Plot Eq. (25) while varying  $p$  from  $1 \rightarrow q$  which Landau level index  $n$  we get

# Landau levels

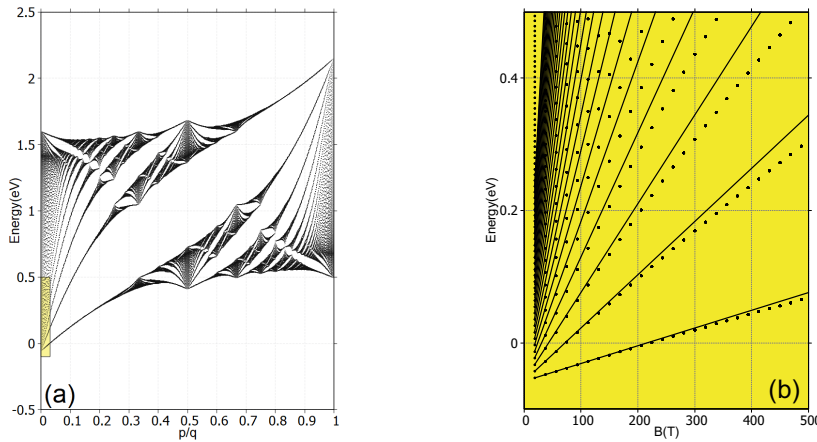
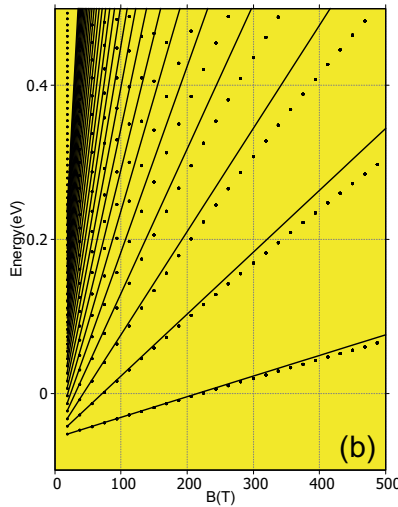


Figure: Landau levels appear in weak magnetic field.

# Landau levels



## Properties

- Increase linearly with respect to  $B$ .
- At weak magnetic field, the Landau levels are well-described.
- Increasing  $B \rightarrow$  fewer filled levels.
- At extremely strong field  $\rightarrow$  only one level is filled.

# The Classical Hall effect

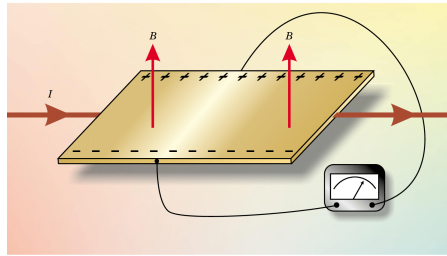
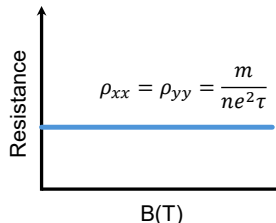


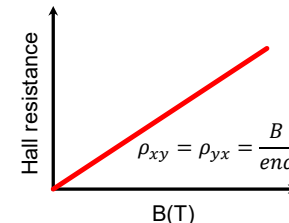
Figure: Classical Hall effect



The Hall effect can be described through Ohm's law

$$\begin{pmatrix} J_x \\ J_y \end{pmatrix} = \begin{pmatrix} \sigma_{xx} & \sigma_{xy} \\ \sigma_{yx} & \sigma_{yy} \end{pmatrix} \begin{pmatrix} E_x \\ E_y \end{pmatrix}, \quad (24)$$

$$\begin{pmatrix} E_x \\ E_y \end{pmatrix} = \begin{pmatrix} \rho_{xx} & \rho_{xy} \\ \rho_{yx} & \rho_{yy} \end{pmatrix} \begin{pmatrix} J_x \\ J_y \end{pmatrix}. \quad (25)$$



# The Quantum Hall effect

It was first discovered in early 1980<sup>[5]</sup>.

The resistance in a MOSFET under a strong magnetic field depicts interesting phenomena.

## Properties

- On Hall plateaux

$$\rho_{xx} = \rho_{yy} = 0, \quad \rho_{xy} = \rho_{yx} = \text{const.}$$

$$\sigma_{xx} = \sigma_{yy} = 0, \quad \sigma_{xy} = \sigma_{yx} = 1/\text{const.}$$

- Between Hall plateaux

$$\rho_{xx}, \rho_{yy} \neq 0 \Rightarrow \sigma_{xx}, \sigma_{yy} \neq 0,$$

$$\rho_{xy} = \frac{R_K}{\nu}, \quad \nu = 1, 2, 3, \dots$$

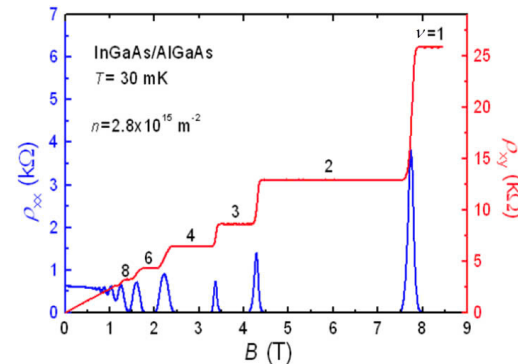


**Figure:** The Quantum Hall effect by Klitzing, Dorda, and Pepper (1980).

# The Quantum Hall effect

The contribution to the Hall conductance is given by

$$\sigma_{xy} = \frac{e^2}{h} \sum_n^{\text{occ.}} \frac{1}{2\pi} \iint_{\text{BZ}} dk_x dk_y \Omega_n^z(\mathbf{k}), \quad (26)$$

since the integral over the Brillouin zone is an integer, we arrived at the TKNN formula<sup>[6]</sup>

$$\sigma_{xy} = \frac{e^2}{h} \nu, \quad \nu = 1, 2, \dots \quad (27)$$

and combine with Streda formula<sup>[7]</sup>

$$\sigma_{xy}(B, E_F) = e \left. \frac{\partial N(E, B)}{\partial B} \right|_{E=E_F}, \quad (28)$$

we have the Diophantine equation

$$r = q \times s_r + p \times \nu_r. \quad (29)$$

[6] Thouless et al., "Quantized Hall Conductance in a Two-Dimensional Periodic Potential".

[7] Streda, "Theory of quantised Hall conductivity in two dimensions".

# The Diophantine equation

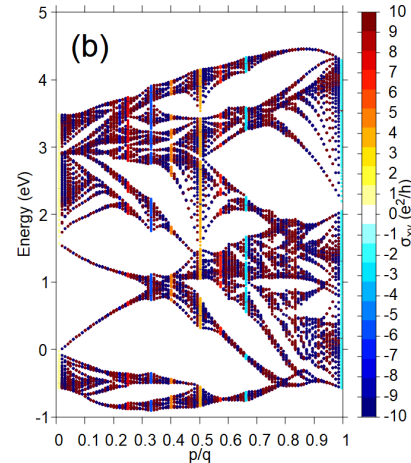
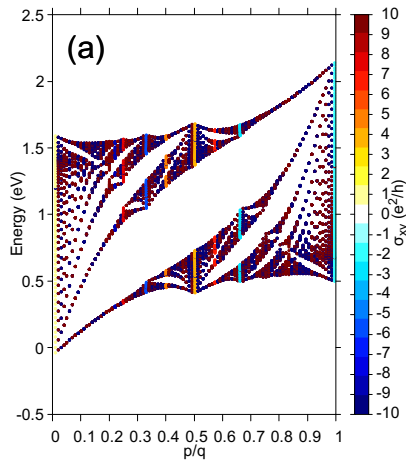
| $r$   | 0 | 1  | 2  | 3  | 4 | 5  | 6  | 7  | 8 | 9  | 10 | 11 | 12 |
|-------|---|----|----|----|---|----|----|----|---|----|----|----|----|
| $\nu$ | 0 | -3 | -6 | 4  | 1 | -2 | -5 | 5  | 2 | -1 | -4 | -6 | 3  |
| $s$   | 0 | 1  | 2  | -1 | 0 | 1  | 2  | -1 | 0 | 1  | 2  | -1 | 0  |

Table: Allowed values of  $r$ .

$$r = q \times s_r + p \times \nu_r.$$

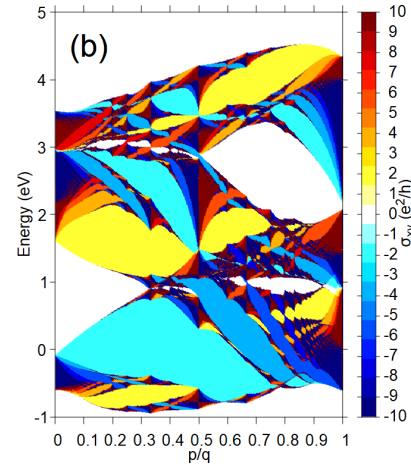
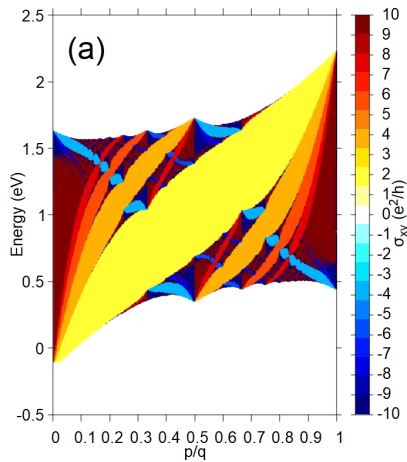
- $p, q$  are the flux number  $\Phi$  and flux quanta  $\Phi_0$ .
- The Chern number  $\nu$  determines the topological and the contribution to the Hall conductance.
- Identifying  $s$  as an index of energy gap in the butterfly.
- $r$  goes from 0 to  $q - 1$  subbands

# Color the butterfly



$$\mathbf{r} = \mathbf{q} \times \mathbf{s}_r + \mathbf{p} \times \mathbf{\nu}_r$$

# Color the butterfly



$$\mathbf{r} = \mathbf{q} \times \mathbf{s}_r + \mathbf{p} \times \mathbf{v}_r$$

## Summary:

- We confirm the Hofstadter butterfly in this model corrected compared to previous study.
- From three-band TB + magnetic field → QHE.

## Further research:

- Fractional Quantum Hall effect
- High Harmonic Generation
- High-order Side-band Generation
- Photovoltaic effect

Thank you for your listening.

## References

- Hofstadter, Douglas R. (1976). "Energy levels and wave functions of Bloch electrons in rational and irrational magnetic fields". In: *Phys. Rev. B* 14 (6), pp. 2239–2249.
- Klitzing, K. v., G. Dorda, and M. Pepper (1980). "New Method for High-Accuracy Determination of the Fine-Structure Constant Based on Quantized Hall Resistance". In: *Phys. Rev. Lett.* 45 (6), pp. 494–497.
- Liu, Gui-Bin et al. (2013). "Three-band tight-binding model for monolayers of group-VIB transition metal dichalcogenides". In: *Phys. Rev. B* 88 (8), p. 085433.
- Radisavljevic, Branimir et al. (2011). "Single-layer MoS<sub>2</sub> transistors". In: *Nature nanotechnology* 6.3, pp. 147–150.
- Streda, P (1982). "Theory of quantised Hall conductivity in two dimensions". In: *Journal of Physics C: Solid State Physics* 15.22, p. L717.
- Thouless, D. J. et al. (1982). "Quantized Hall Conductance in a Two-Dimensional Periodic Potential". In: *Phys. Rev. Lett.* 49 (6), pp. 405–408.